First-Principles Calculation for the Influence of C and O on the Mechanical Properties of γ-TiAl Alloy at High Temperature

Jiahua Wang, Yong Lu and Xiaohong Shao *

College of Science, Beijing University of Chemical Technology, Beijing 100029, China;
2016200907@mail.buct.edu.cn (J.W.); luy@mail.buct.edu.cn (Y.L.)
* Correspondence: shaoxh@mail.buct.edu.cn; Tel.: +86-10-6443-3867

Abstract: The elastic constants of temperature dependence, thermal expansion coefficient and phonon dispersion relations of γ-TiAl doped with C/O have been investigated using first-principles calculations in order to gain insight into the mechanical performance of γ-TiAl in cases of high temperature. This study shows that γ-TiAl maintains stability at high temperatures introduced by C or O atoms. Importantly, the hardness increases and retains excellent resistance to external pressure. The results indicate that even if the TiAl alloy is doped with C or O atoms, it can also exhibit excellent mechanical properties at a high temperature.

Keywords: first-principles calculation; mechanical properties; TiAl alloy

1. Introduction

γ-TiAl alloys have received much attention for their broad application prospects in the aerospace, automotive, chemical and marine industries because of their low density, high specific strength and stiffness, high resistance to high temperature creep, oxidation and hydrogen embrittlement [1–5].

Duwez et al. [6] first reported the existence of a Ti-Al phase in titanium-aluminum binary systems and determined it structure. This laid a foundation for subsequent research. In order to gain a deeper understanding of the mechanical properties of γ-TiAl, more detailed research on basic properties is required, such as structural features, elastic behavior, phase stability and so on. Hsieh et al. [7] explored the structural characteristics of γ-TiAl. Erdely et al. [8] and Huang et al. [9] studied the changes in microstructure of γ-TiAl at high temperature. Tanaka et al. [10,11] and He et al. [12] measured the elastic constants of γ-TiAl at different temperatures and described the experimental procedures. In theory, some studies [13–17] have qualitatively analyzed the phase stability, structural deformation and effects of oxygen impurity of γ-TiAl by first-principles calculations. Fu et al. [18] and Zhang et al. [19] explored the mechanical and thermodynamic properties of γ-TiAl under high pressure. However, there is little theoretical research to evaluate the influence of temperature on γ-TiAl, which cannot truly reflect the performance of γ-TiAl in practical applications. In addition, the γ-TiAl phase provides many of the qualities required in innovative structural high temperature and marine applications. The evolution of elastic properties upon temperature and resistance to microbial corrosion (C, O, P, S, etc.) are similarly important [20–26]. Moreover, during the preparation of the alloy, oxygen and carbon atoms are easily absorbed into γ-TiAl, which affects the use of γ-TiAl. Therefore, this work is mainly to study the effect of oxygen and carbon impurities on the mechanical properties of γ-TiAl alloy at high temperature.

In this work, we obtained the temperature dependent elastic modulus by the combination of density functional perturbation theory (DFPT), quasi-harmonic approximation (QHA) method

and continuum elasticity theory. Likewise, the thermal stability of γ-TiAl with oxygen and carbon impurities were analyzed by calculating the phonon dispersion curves. We showed that the interaction between individual orbital electrons of the impurity and the electrons of Ti and Al atoms by analyzing the partial densities of their respective states. These data will be helpful to the practical application of γ-TiAl alloy in the future.

2. Computational Details

According to the QHA method [27,28], the Helmholtz free energy can be expressed as: $E(V,T) = E_{static}(V) + E_{phon}(V,T) + E_{elec}(V,T)$, where $E_{static}(V)$ is the total energy at 0 K, $E_{phon}(V,T)$ is the phonon free energy and $E_{elec}(V,T)$ is the thermal electronic contribution to the free energy. $E_{static}(V)$ and $E_{elec}(V,T)$ can be calculated by first-principles calculations directly. Because γ-TiAl belongs to the tetragonal crystal, the six independent elastic constant deformation models of C_{11}, C_{12}, C_{13}, C_{33}, C_{44}, C_{66} can be defined by the formula [29]: $E(V,\delta) = E(V_0,0) + V_0[\sum_i \tau_i \delta_i \xi_i + \frac{1}{2}\sum_{i,j} C_{ij}\delta_i\xi_i\delta_j\xi_j]$,

where $E(V,\delta)$ is the total energy for the system with respect to a small strain δ on the equilibrium cell. $E(V_0,0)$ and V_0 are the total energy and volume of the equilibrium cell without strains, respectively. τ_i is an element in the stress tensor. $\xi_{i/j}$ is a factor of the Voigt index [30] and $\delta_{i/j}$ is the small strain applied on the equilibrium cell. The sets of distortions were selected as $(\delta; \delta; 0; 0; 0; 0)$, $(\delta; -\delta; 0; 0; 0; 0)$, $(0; 0; \delta; 0; 0; 0)$, $(0; 0; 0; \delta; 0; 0)$, $(\delta; \delta; \delta; 0; 0; 0)$, $(0; 0; 0; 0; 0; \delta)$ on the equilibrium cell with a small strain δ varying from -0.03 to 0.03 in steps of 0.006, which has used in our previous work [31]. The elastic constants can be calculated by the equations: $C_{11} + C_{12} = \frac{D_1}{2}$, $C_{11} - C_{12} = \frac{D_2}{2}$, $C_{33} = D_3$, $C_{44} = \frac{D_4}{4}$, $2(C_{11} + C_{12} + 2C_{13}) + C_{33} = D_5$ and $C_{66} = D_6$, where $D_i(i = 1–6)$ represents the second-order strain derivatives of the Helmholtz free energy under the above six kinds of deformation forms, respectively.

The structural optimization and mechanical properties were calculated using first principles calculations based on density functional theory (DFT) [32,33] in the Vienna Ab initio Simulation Package (VASP) code [34]. The ion-electron interaction was expressed by the projector augmented wave (PAW) method [35]. The exchange correlation energy of the electrons is described by generalized gradient approximation (GGA) with the Perdew-Burke-Ernzerhof (PBE) [36,37] form. The energy cutoff was set to 600 eV and the Brillouin-zone (BZ) sampling was performed for $7 \times 7 \times 7$ k-point Monkhorst-Pack mesh [38]. The self-consistent convergence of the total energy was set to 10^{-6} eV/atom and the maximum force on the atom was below 10^{-5} eV/Å. In this work, we used the $2 \times 2 \times 2$ supercell containing 16 Ti and 16 Al atoms, respectively. The concentrations of C and O are both set to 3.03 at%, which is below the solubility limit of C/O in TiAl lattice [16,17]. The kinetic stability was discussed using the phonon spectra calculations in PHONOPY code [39].

3. Results and Discussion

In our previous work [31], especially for two equivalent types of the pentahedral (P_1, P_2) sites and octahedral (O_1, O_2) sites, the ideal positions have been determined by comparing the formation energy of the sites. The ideal positions of C and O atoms in the γ-TiAl alloy have been optimized and shown in Figure 1. The solution sites of the C atoms are in the O position of the octahedral center, and the O atoms are in the P position of the pentahedral center, respectively. The Helmholtz free energy in different crystal volumes at finite temperature was calculated by using the QHA method (see Figure 2). Equilibrium volume can be obtained by fitting the data to the Vinet equation of states for each temperature. It can be found that the equilibrium volume increases with increasing temperature. The relationship of volume and temperature is shown in Figure 3. As is seen, the volume of TiAlO is larger than that of TiAlC at different temperatures. The constant volume thermal expansion is shown in Figure 4. When the temperature is higher than 100 K, the two lines are separated and the thermal expansion coefficient of TiAlO is gradually larger than that of TiAlC. At 850 K, the thermal expansion coefficient for TiAlC is about $3.64 \times 10^{-5} K^{-1}$ and for TiAlO is about $3.80 \times 10^{-5} K^{-1}$. Both values are larger than the $3.55 \times 10^{-5} K^{-1}$ value of pure γ-TiAl [31], indicating that C and O atoms easily

make γ-TiAl deform at high temperature. In order to analyze the stability of TiAlC and TiAlO at different temperatures, we calculated the phonon dispersion curves at 0 K, 300 K, and 850 K as shown in Figure 5. Obviously, there are no unstable branches with negative vibrational frequencies, indicating that TiAlO and TiAlC are dynamically stable.
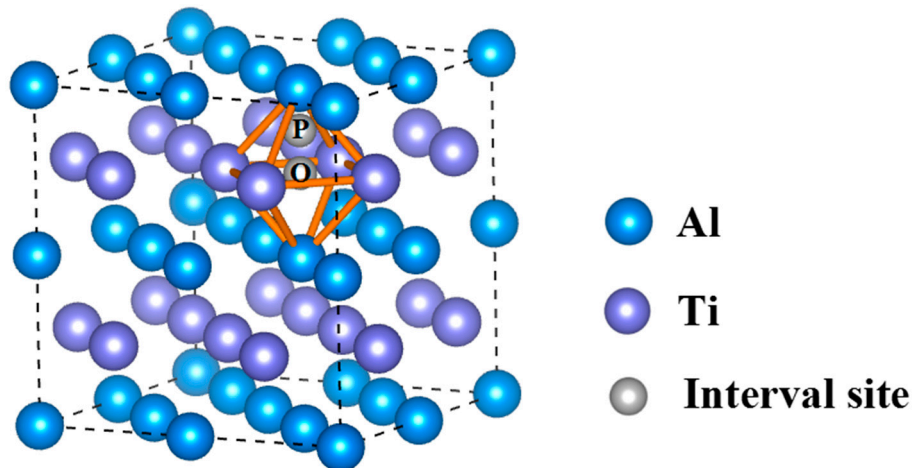

Figure 1. A 2 × 2 × 2 supercell of γ-TiAl matrix marked with the pentahedron (P) site and octahedral (O) site represented as gray spheres, where Ti atoms are represented as purple spheres and Al atoms are represented as blue spheres.
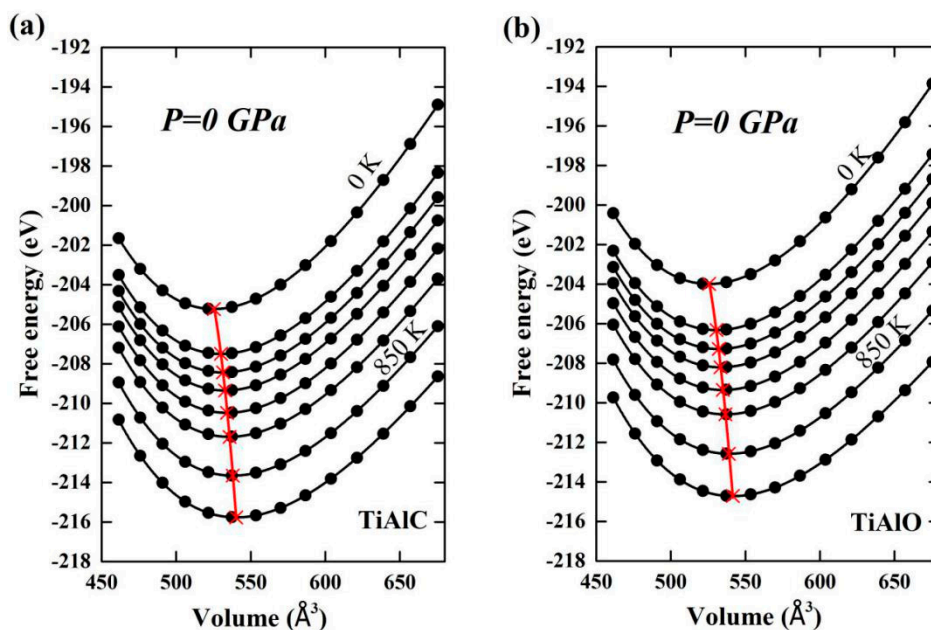

Figure 2. Volume-dependent Helmholtz free energy of TiAlC (**a**) and TiAlO (**b**). Red lines connect the equilibrium volume with the minimum free energy at every temperature, where red cross indicates the equilibrium volume of each temperature.
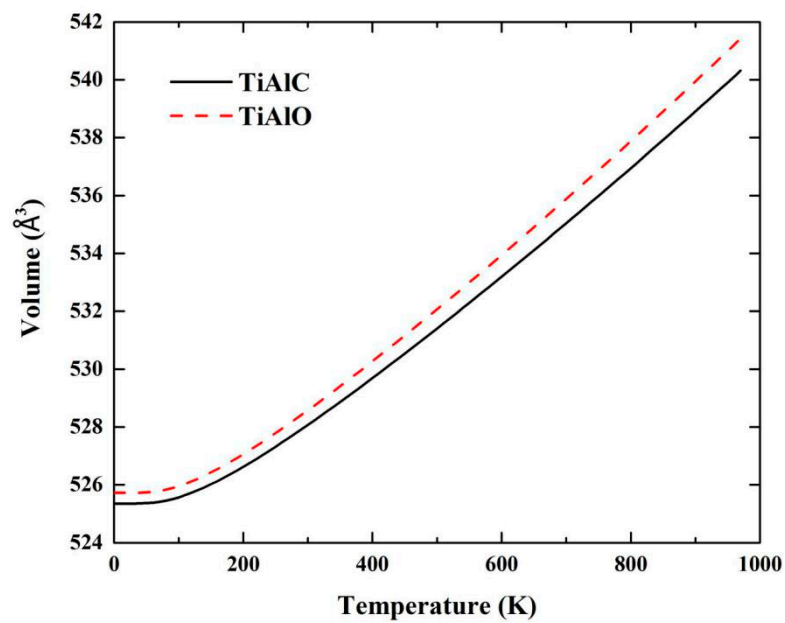
Figure 3. Volumetric expansion as a function of temperature for TiAlC and TiAlO, where the solid line represents TiAlC and the dashed line represents TiAlO.
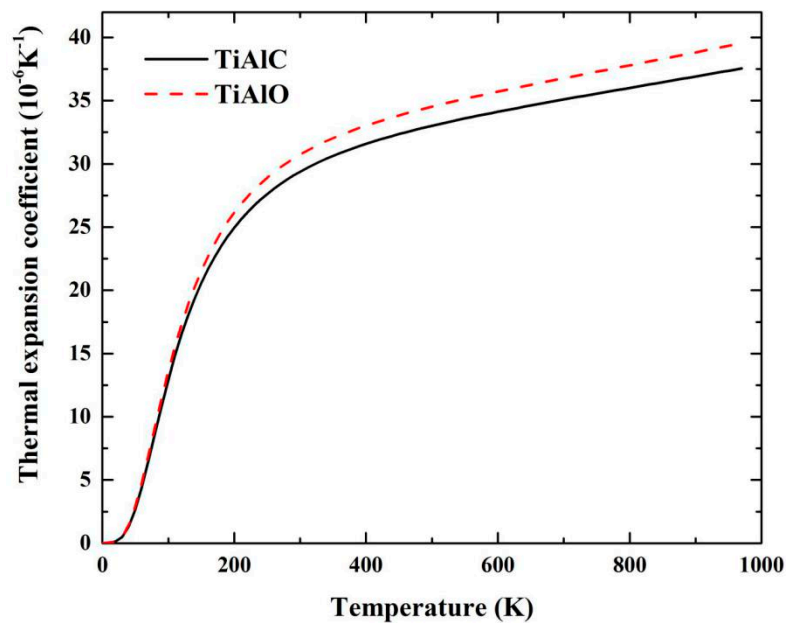

Figure 4. The volume thermal expansion coefficient as a function of temperature, where the solid line represents TiAlC and the dashed line represents TiAlO.
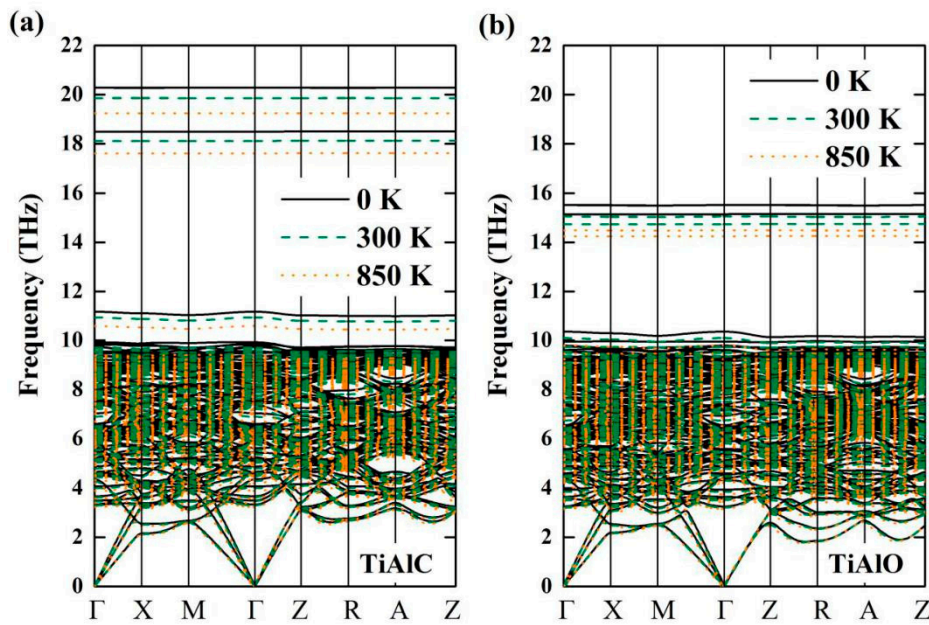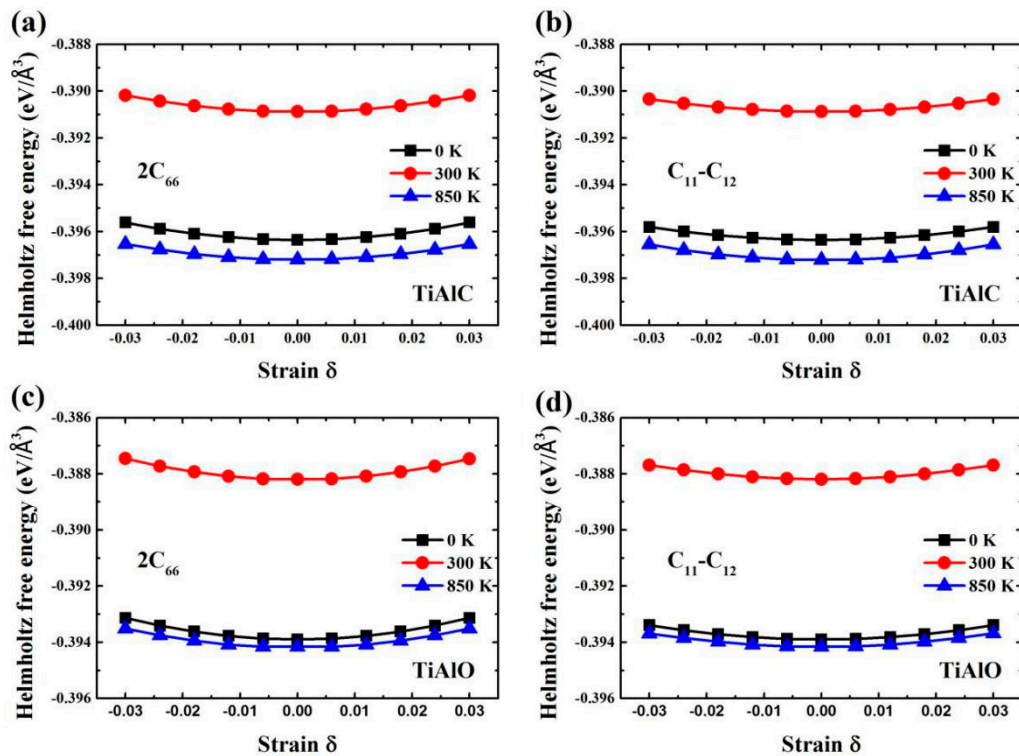
Figure 5. Phonon dispersion relations of TiAlC (**a**) and TiAlO (**b**) along high-symmetry q points in Brillouin zone at 0 K, 300 K, and 850 K, respectively.

The elastic constant can be thought of as the strain derivative of the Helmholtz free energy [40,41]. We derived the elastic constants from the second order coefficients by polynomial fitting the Helmholtz free energy densities to strain. The relationship between Helmholtz free energy and strain δ upon temperature for C_{11}-C_{12} and C_{66} is shown in Figure 6. It shows that the energy curve changes significantly with the increases of temperature and strain. The elastic constants at different temperatures are listed in Table 1. For comparison, the temperature is chosen as same to our previous work [31]. The mechanical stability criteria [42] for tetragonal crystal of $C_{11} > |C_{12}|$, $2C_{13}^2 < C_{33}(C_{11} + C_{12})$, $C_{44} > 0$, $C_{66} > 0$ is applied for stability analysis. More importantly, γ-TiAl alloy can maintain excellent mechanical properties doped with C/O atoms. Most of the elastic constants are generally reduced with temperature. However, C_{11}, C_{66} of TiAlC and C_{12} of TiAlO have a significant increase at 620 K.

Table 1. The calculated elastic constants of TiAlC and TiAlO at different temperatures.

Phase	Temperature (K)	C_{11} (GPa)	C_{12} (GPa)	C_{13} (GPa)	C_{33} (GPa)	C_{44} (GPa)	C_{66} (GPa)
TiAl	0 [a]	171.6	89.7	91.3	172.2	114.5	65.4
	0 [b]	164	85.5	81.04	178.57	109.6	72.6
	0 [c]	167.4	87.7	86.1	164.2	111.1	73.7
	0 [d]	187	74.8	74.8	182	109	81.2
	298 [d]	183	74.1	74.4	178	105	78.4
	300 [e]	186	72	74	176	101	77
	300 [a]	161.2	88.2	91.3	157.8	109.6	65.7
	410 [a]	157.7	87.2	91.4	149.3	108.4	65.3
	500 [a]	158.8	81.0	93.2	145.4	107.2	65.1
	620 [a]	152.9	80.8	95.9	144.1	104.7	68.9
	740 [a]	151.1	79.0	96.1	137.0	103.3	63.0
	850 [a]	148.0	82.4	95.4	133.3	101.7	62.5
TiAlC	0	191.0	92.4	87.6	181.9	109.5	66.0
	300	181.9	85.9	85.8	169.9	102.7	62.3
	410	178.8	84.2	85.4	166.1	100.7	61.2
	500	175.1	81.9	84.5	161.4	98.2	59.7
	620	178.1	78.9	83.1	155.3	98.3	62.2
	740	175.4	76.8	80.7	160.6	95.5	61.2
	850	171.9	74.8	79.7	156.1	93.0	59.2
TiAlO	0	181.4	91.5	92.3	172.4	109.7	68.2
	300	173.8	84.4	88.2	164.9	103.0	66.3
	410	171.2	82.5	87.1	162.8	101.1	65.3
	500	164.4	71.6	94.4	161.8	106.9	69.3
	620	162.5	78.2	86.0	156.0	96.6	60.4
	740	161.4	76.8	83.9	157.2	95.9	61.8
	850	158.9	74.4	84.3	150.9	94.3	60.7

[a] [31]; [b] [18]; [c] [19]; [d] [11]; [e] [12].

Figure 6. The relationship between Helmholtz free energy and strain δ upon temperature for (**a**) C_{11}-C_{12} of TiAlC, (**b**) C_{66} of TiAlC, (**c**) C_{11}-C_{12} of TiAlO and (**d**) C_{66} of TiAlO, respectively.

The bulk modulus (*B*), shear modulus (*G*), Young's modulus (*E*) and Poisson's ratio (*ν*) can be calculated by using the following equations [43]: $B = \frac{1}{2}(B_V + B_R)$, $G = \frac{1}{2}(G_V + G_R)$, $E = \frac{9GB}{(3B+G)}$ and $v = \frac{(3B-2G)}{[2(3B+G)]}$, where subscript *V* denotes the Voigt bound and *R* denotes the Reuss bound [43–45]. The data are listed in Table 2 and are shown in Figure 7. There are some fluctuations in these data, which may be caused by the limitations of the QHA method. The same phenomenon can be found in some thermodynamic calculations of metals [27,46–48]. In addition, only a small part of the range causes fluctuations, which will not affect the entire trend. From Table 2, as the temperature increases from 0 K to 850 K, *B*, *G* and *E* of TiAlC decrease by 12%, 13%, 12%, while they decrease by 12%, 13%, 13% for TiAlO, respectively. The *B*, *G* and *E* of pure γ-TiAl decrease by 8%, 22%, 20% respectively and *ν* increase from 0.258 to 0.290 [31]. Although the incorporation of C or O atoms deteriorates the decline of *B* for γ-TiAl, it is excellent to improve *G* and *E* of γ-TiAl. In addition, the *B* of TiAlC and TiAlO are 107.51 GPa and 106.09 GPa at 850 K, respectively, which is similar to the *B* of γ-TiAl (108.4 GPa). This indicates that γ-TiAl doped with C/O atoms also keep strong resistance to external pressure at high temperature. However, the Poisson's ratio decreases significantly for TiAlC and TiAlO compared with pure γ-TiAl.

Table 2. The calculated elastic modulus, including the bulk modulus (*B*), shear modulus (*G*), Young's modulus (*E*), Poisson's ratio (*ν*), and *G/B* of TiAlC and TiAlO at different temperatures (K).

Phase	Temperature (K)	*B* (GPa)	*G* (GPa)	*E* (GPa)	*ν*	*G/B*
TiAl	0 [a]	117.8	67.9	171.1	0.258	0.576
	0 [b]	110.69	68.57	170.50	0.26	0.619
	0 [c]	113.1	68.1	170.2	0.249	0.602
	0 [d]	111.64	78.36	190.51	0.216	0.702
	298 [d]	109.97	75.68	184.67	0.220	0.688
	300 [e]	109.76	74.83	182.92	0.222	0.682
	300 [a]	113.5	62.9	159.4	0.266	0.554
	410 [a]	111.6	60.8	154.3	0.269	0.545
	500 [a]	110.9	60.1	152.5	0.271	0.541
	620 [a]	110.5	57.6	147.2	0.278	0.521
	740 [a]	109.1	54.7	140.5	0.285	0.501
	850 [a]	108.4	52.9	136.6	0.290	0.488
TiAlC	0	122.0	72.2	180.9	0.253	0.592
	300	116.5	67.6	169.9	0.257	0.580
	410	114.8	66.1	166.3	0.259	0.576
	500	112.5	64.3	162.0	0.260	0.571
	620	111.1	65.2	163.6	0.253	0.587
	740	109.7	65.0	162.8	0.253	0.593
	850	107.5	63.1	158.4	0.254	0.587
TiAlO	0	120.8	68.9	173.7	0.260	0.571
	300	114.9	66.0	166.1	0.259	0.574
	410	113.1	64.9	163.5	0.259	0.574
	500	112.1	64.5	162.3	0.259	0.575
	620	109.0	60.9	154.1	0.265	0.559
	740	107.7	61.5	155.0	0.260	0.571
	850	106.1	59.7	150.8	0.263	0.563

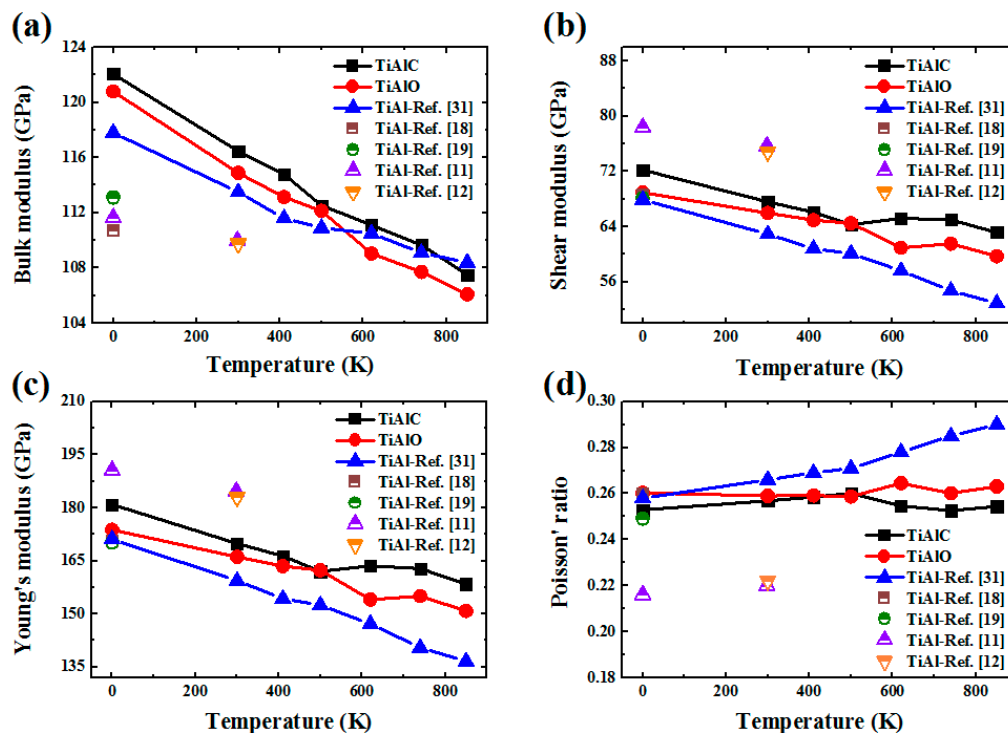[a] [31]; [b] [18]; [c] [19]; [d] [11]; [e] [12].

Figure 7. The calculated temperature dependent elastic modulus of (**a**) bulk modulus (*B*), (**b**) shear modulus (*G*), (**c**) Young's modulus (*E*), and (**d**) Poisson's ratio (*ν*) for TiAlC, TiAlO and pure γ-TiAl.

As is shown in Figure 7a–c, all the modulus of the TiAlC and TiAlO phases are decreasing along with the increase of temperature in the range of 0 K to 500 K. In addition, the modulus of TiAlC and TiAlO is higher than that of γ-TiAl alloy before 500 K. The phenomenon indicates that the resisting compression and shear deformation of γ-TiAl can be improved by appropriately adding O atoms below 500 K. Up to 500 K, the bulk modulus of the TiAlC and TiAlO phase continues to decrease, while the other modulus have significant variations. The bulk modulus of TiAlO is significantly lower than that of γ-TiAl, while the other modulus of TiAlC and TiAlO remain higher than that of γ-TiAl, indicating that O has a greater effect on γ-TiAl to resist external pressure above 500 K. In Figure 7d, the *ν* of TiAlO gradually decreases, while the *ν* of TiAlC gradually increases below 500 K and they have rebound trends above 500 K.

It is known that the bulk modulus or shear modulus can measure hardness in an indirect way and Young's modulus is generally used to provide a measure of solid stiffness [49–52]. Poisson's ratio can provide more information about the binding characteristics than other elastic constants [50]. The smaller the Poisson's ratio, the better the crystal's shear stability. From Table 2, it can be found that the incorporation of C and O atoms can increase the shear stability of γ-TiAl alloy. In addition, the high (low) *G*/*B* value is related to the brittleness (ductility) of the material and the critical value of the separation ductility, and brittle material is about 0.57 [52]. In Table 2, the values of *G*/*B* of TiAlC are all greater than 0.57. Therefore, the toughness can be decreased and the brittleness can be increased for γ-TiAl doped with C. For TiAlO, it is less than 0.57 at temperatures ranging from 620–850 K. The other is around 0.57, showing that the ductility can be weakened and the brittleness can be increased for the γ-TiAl doped with O. In general, the ductility of the γ-TiAl alloy doped with C/O atoms can be impaired, but its hardness can be enhanced.

Previous studies [53,54] have proven that the mechanical properties of TiAl alloys are related to chemical bonds. The Ti(3d)-Al(3p) covalent bonds can present a large barrier to the plastic deformation and weaken the ductility of the TiAl alloy, due to the strong bonding directionality [53,54]. The partial density of states is plotted in Figure 8. As is seen in Figure 8a, the 3d orbital electrons of Ti play a dominant role. The 3d orbital electrons of the Ti atoms and the 3p orbital electrons of Al atoms show

obvious hybridization at the Fermi energy level. From Figure 8b, we can see that the γ-TiAl alloy exhibits an electronic state at −11.39 eV, and the 3d-Ti orbitals and the 3p- and 3s-Al orbitals hybridize with the 2s-C orbitals, indicating that there is a new energy state (bonding state) and strengthen Ti(3d)-Al(3p) covalent bonds. In addition, the number of 3p-Al orbital electrons increase slightly and the number of 3d-Ti orbital electrons still maintain a high value at the Fermi energy level. In Figure 8c, the electronic density of states occurs at −8.64 eV. However, the 3s-Al orbitals and the 2p-O orbitals have a significant hybridization and the energy range of hybridization is −9 to −5 eV, which indicates that a new energy state (bonding state) is formed here. Further, the number of 3p-Al orbital electrons and 3d-Ti orbital electrons have similar changes to TiAlC at the Fermi energy level, indicating that Ti(3d)-Al(3p) covalent bonds can be enhanced at the Fermi energy level because of the incorporation of C and O atoms. In summary, since the hybridization strength of TiAlC is higher than that of TiAlO, the increase in hardness of γ-TiAl alloy by the C atom is more obvious. Although the hybridization of TiAlO is weak, the hybridization range is relatively wide. Therefore, the hardness of the γ-TiAl alloy is also improved. In addition, the incorporation of the C or O atoms lead to an increase in the hybridization strength of 3d-Ti orbital electrons and 3p-Al orbital electrons, which results in an enhancement in the Ti(3d)-Al(3p) covalent bonds. Therefore, there is an increase in brittleness and a decrease in ductility of the γ-TiAl alloy.
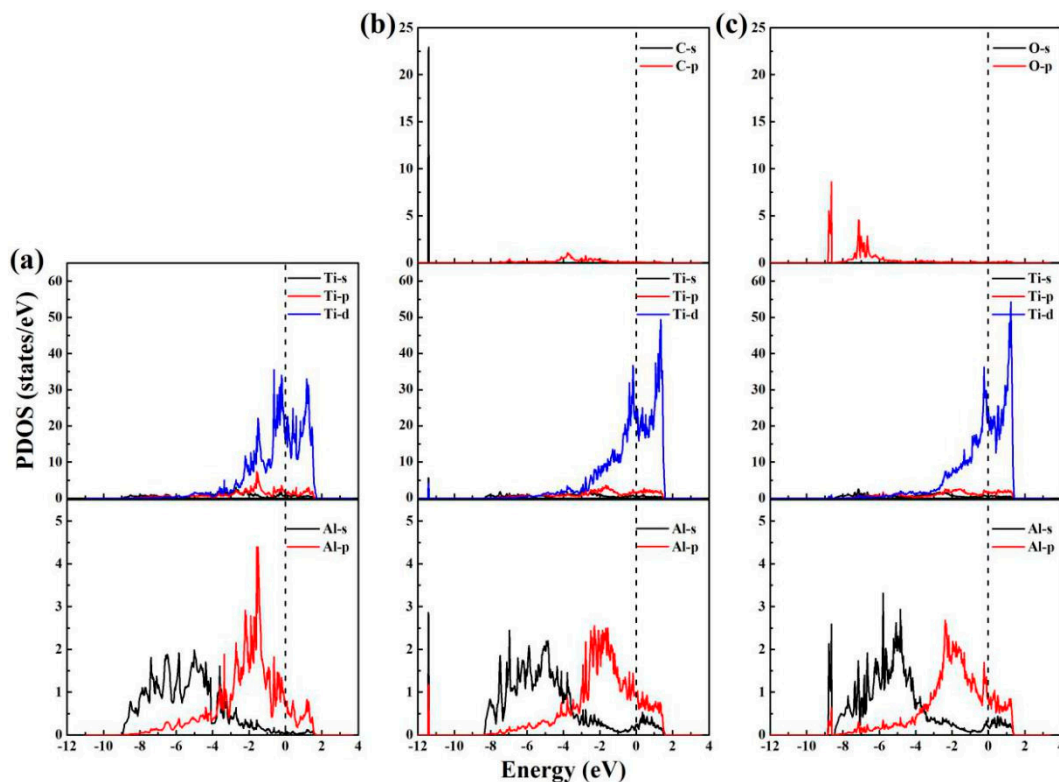

Figure 8. The partial densities of states of pure γ-TiAl (**a**), TiAlC (**b**), TiAlO (**c**).

4. Conclusions

We have studied the effects of C and O atoms on the mechanical properties of γ-TiAl at high temperature by combining first-principles calculations, QHA methods and continuous elastic theory. The phonon dispersion curves show that TiAlC and TiAlO are dynamically stable. The B, E, G and ν of TiAlC and TiAlO show that the incorporation of C and O atoms can increase the hardness of the γ-TiAl alloy and maintain excellent resistance to external pressure at high temperature. However, the ductility of the γ-TiAl alloy is gradually weakened and the brittleness is gradually increased. By analyzing the hybridization between the orbital electrons of each atom in PDOS, the hybridization strength of

TiAlC is higher than that of TiAlO, which results in a greater improvement of hardness. Meanwhile, C and O atoms lead to an enhancement in the Ti(3d)-Al(3p) covalent bonds so that the ductility of the γ-TiAl alloy is reduced. Although C and O atoms weaken the ductility of the γ-TiAl, it can still maintain excellent mechanical properties at high temperature.

Author Contributions: X.S. and Y.L. conceived and designed the researchs; J.W. performed the researchs; J.W. and X.S. analyzed the data; X.S. contributed the analysis tools; J.W. wrote the paper.

Conflicts of Interest: The authors declare no conflicts of interest.

References

1. Kumpfert, J.; Kim, Y.W.; Dimiduk, D.M. Effect of microstructure on fatigue and tensile properties of the gamma TiAl alloy Ti-46.5Al-3.0Nb-2.1Cr-0.2W. *Mater. Sci. Eng. A* **1995**, *192–193*, 465–473. [CrossRef]
2. Mishin, Y.; Herzig, C. Diffusion in the Ti–Al System. *Acta Mater.* **2000**, *48*, 589–623. [CrossRef]
3. Wallgram, W.; Schmölzer, T.; Cha, L.; Das, G.; Güther, V.; Clemens, H. Technology and mechanical properties of advanced γ-TiAl based alloys. *Int. J. Mater. Res.* **2009**, *100*, 1021–1030. [CrossRef]
4. Appel, F.; Clemens, H.; Oehring, M. Recent Advances in Development and Processing of Titanium Aluminide Alloys. *Mat. Res. Soc. Symp. Proc.* **2001**, *646*. [CrossRef]
5. Chen, G.; Peng, Y.; Zheng, G.; Qi, Z.; Wang, M.; Yu, H.; Dong, C.; Liu, C.L. Polysynthetic twinned TiAl single crystals for high-temperature applications. *Nat. Mater.* **2016**, *15*, 876. [CrossRef] [PubMed]
6. Duwez, P.; Taylor, J.L. Crystal Structure of TiAl. *JOM* **1952**, *4*, 70–71. [CrossRef]
7. Hsieh, K.-C.; Austinchang, Y.; Freeman, A.J.; Oguchi, T.; Xu, J.-H. Thermodynamic and structural parameters of the body-center tetragonal TiAl phase. *Scr. Metall.* **1988**, *22*, 1267–1272. [CrossRef]
8. Erdely, P.; Stark, A.; Clemens, H.; Mayer, S. In-situ High-energy X-ray Diffraction on an Intermetallic β-stabilised γ-TiAl Based Alloy. *BHM* **2015**, *160*, 221–225. [CrossRef]
9. Huang, Z.W.; Lin, J.P.; Sun, H.L. Microstructural changes and mechanical behaviour of a near lamellar γ-TiAl alloy during long-term exposure at 700 °C. *Intermetallics* **2017**, *85*, 59–68. [CrossRef]
10. Tanaka, K.; Koiwa, M. Single-crystal elastic constants of intermetallic compounds. *Intermetallics* **1996**, *4*, S29–S39. [CrossRef]
11. Tanaka, K.; Ichitsubo, T.; Inui, H.; Yamaguchi, M.; Koiwa, M. Single-crystal elastic constants of γ-TiAl. *Philos. Mag. Lett.* **1996**, *73*, 71–78. [CrossRef]
12. He, Y.; Schwarz, R.B.; Darling, T.; Hundley, M.; Whang, S.H.; Wang, Z.M. Elastic constants and thermal expansion of single crystal γ-TiAl from 300 to 750 K. *Mater. Sci. Eng. A* **1997**, *239–240*, 157–163. [CrossRef]
13. Zou, J.; Fu, C.L.; Yoo, M.H. Phase stability of intermetallics in the Al-Ti system: A first-principles total-energy investigation. *Intermetallics* **1995**, *3*, 265–269. [CrossRef]
14. Tang, P.-Y.; Huang, G.-H.; Xie, Q.-L.; Li, J.-Y. Ideal shear strength and deformation behaviours of L1$_0$ TiAl from first-principles calculations. *Bull. Mater. Sci.* **2016**, *39*, 1411–1418. [CrossRef]
15. Liu, Y.L.; Liu, L.M.; Wang, S.Q.; Ye, H.Q. First-principles study of shear deformation in TiAl and Ti$_3$Al. *Intermetallics* **2007**, *15*, 428–435. [CrossRef]
16. Liu, Y.; Chen, K.; Zhang, J.; Hu, Z.; Lu, G.; Kioussis, N. Electronic effects of oxygen and vanadium impurities in TiAl. *J. Phys. Condens. Matter* **1997**, *9*, 9829–9843. [CrossRef]
17. Zhou, H.-B.; Wei, Y.; Liu, Y.-L.; Zhang, Y.; Lu, G.-H. First-principles investigation of site preference and bonding properties of alloying element in TiAl with O impurity. *Modell. Simul. Mater. Sci. Eng.* **2010**, *18*, 015007. [CrossRef]
18. Fu, H.; Zhao, Z.; Liu, W.; Peng, F.; Gao, T.; Cheng, X. Ab initio calculations of elastic constants and thermodynamic properties of γTiAl under high pressures. *Intermetallics* **2010**, *18*, 761–766. [CrossRef]
19. Zhang, C.; Hou, H.; Zhao, Y.; Yang, X.; Guo, Y. First-principles study on structural, elastic and thermal properties of γ-TiAl and α$_2$-Ti$_3$Al phases in TiAl-based alloy under high pressure. *Int. J. Mod. Phys. B* **2017**, *31*, 1750079. [CrossRef]
20. Zhang, Z.G.; Peng, Y.P.; Mao, Y.L.; Pang, C.J.; Lu, L.Y. Effect of hot-dip aluminizing on the oxidation resistance of Ti-6Al-4V alloy at high temperatures. *Corros. Sci.* **2012**, *55*, 187–193. [CrossRef]

21. Cheng, J.; Li, F.; Zhu, S.; Yu, Y.; Qiao, Z.; Yang, J. Electrochemical corrosion and tribological evaluation of TiAl alloy for marine application. *Tribol. Int.* **2017**, *115*, 483–492. [CrossRef]

22. Du, H.L.; Datta, P.K.; Burnell-gray, J.S.; Lewis, D.B. Effect of Nb coating on the sulphidation/oxidation behaviour of Ti and Ti-6Al-4V alloy. *J. Mater. Sci.* **1995**, *30*, 2640–2647. [CrossRef]

23. Pedersen, A.; Hermansson, M. Inhibition of Metal Corrosion by Bacteria. *Biofouling* **1991**, *3*, 1–11. [CrossRef]

24. Lei, F.; Liu, L.; Yu, Z.; Gao, M.; Li, Y.; Wang, F. Corrosion Behavior of Ti60 Alloy under a Solid NaCl Deposit in a Wet Oxygen Flow at 600 °C. *Sci. Rep.* **2016**, *6*, 29019.

25. Wu, X.; Hu, D.; Loretto, M.H. Alloy and process development of TiAl. *J. Mater. Sci.* **2004**, *39*, 3935–3940. [CrossRef]

26. Zhang, W.; Gao, L.; Li, J.; Yang, B.; Yin, Y. TiAl/B_4C marine material-Fabrication, mechanical and corrosion properties. *Ceram. Int.* **2011**, *37*, 783–789. [CrossRef]

27. Wang, Y.; Liu, Z.-K.; Chen, L.-Q. Thermodynamic properties of Al, Ni, NiAl, and Ni_3Al from first-principles calculations. *Acta Mater.* **2004**, *52*, 2665–2671. [CrossRef]

28. Guo, Z.-C.; Luo, F.; Zhang, X.-L.; Yuan, C.-Y.; Lin, C.-A.; Cai, L.-C. First-principles calculations of elastic, phonon and thermodynamic properties of W. *Mol. Phys.* **2016**, *114*, 3430–3436. [CrossRef]

29. Fast, F.; Wills, J.M.; Johansson, B.; Eriksson, O. Elastic constants of hexagonal transition metals: Theory. *Phys. Rev. B* **1995**, *51*, 17431–17438. [CrossRef]

30. Voigt, W. *Lehrburch der Kristallphys*; Vieweg + Teubner Verlag: Leipzig, Germany, 1928.

31. Wang, J.-H.; Lu, Y.; Zhang, X.-L.; Shao, X.-H. The elastic behaviors and theoretical tensile strength of γ-TiAl alloy from the first principles calculations. *Intermetallics* **2018**, *101*, 1–7. [CrossRef]

32. Hohenberg, P.; Kohn, W. Inhomogeneous Electron Gas. *Phys. Rev.* **1964**, *136*, B864–B871. [CrossRef]

33. Kohn, W.; Sham, L.J. Self-consistent Equations Including Exchange and Correlation Effects. *Phys. Rev.* **1965**, *140*, A1133–A1138. [CrossRef]

34. Kresse, G.; Furthmüller, J. Efficient iterative schemes for ab initio total-energy calculations using a plane-wave basis set. *Phys. Rev. B* **1996**, *54*, 11169–11186. [CrossRef]

35. Blöchl, P.E. Projector augmented-wave method. *Phys. Rev. B* **1994**, *50*, 17953–17979. [CrossRef]

36. Perdew, J.P.; Burke, K.; Ernzerhof, M. Generalized Gradient Approximation Made Simple. *Phys. Rev. Lett.* **1996**, *77*, 3865–3868. [CrossRef] [PubMed]

37. Hammer, B.; Hansen, L.B.; Nørskov, J.K. Improved adsorption energetics within density-functional theory using revised Perdew-Burke-Ernzerhof functionals. *Phys. Rev. B* **1999**, *59*, 7413–7421. [CrossRef]

38. Monkhorst, H.J.; Pack, J.D. Special points for Brillouin-zone integrations. *Phys. Rev. B* **1976**, *13*, 5188–5192. [CrossRef]

39. Togo, A.; Oba, F.; Tanaka, I. First-principles calculations of the ferroelastic transition between rutile-type and $CaCl_2$-type SiO_2 at high pressures. *Phys. Rev. B* **2008**, *78*, 134106. [CrossRef]

40. Zhao, J.; Winey, J.M.; Gupta, Y.M. First-principles calculations of second-and third-order elastic constants for single crystals of arbitrary symmetry. *Phys. Rev. B* **2007**, *75*, 094105. [CrossRef]

41. Shao, T.; Wen, B.; Melnik, R.; Yao, S.; Kawazoe, Y.; Tian, Y. Temperature dependent elastic constants for crystals with arbitrary symmetry: Combined first principles and continuum elasticity theory. *J. Appl. Phys.* **2012**, *111*, 083525. [CrossRef]

42. Mouhat, F.; Coudert, F.-X. Necessary and sufficient elastic stability conditions in various crystal systems. *Phys. Rev. B* **2014**, *90*, 224104. [CrossRef]

43. Wu, Z.-J.; Zhao, E.-J.; Xiang, H.-P.; Hao, X.-F.; Liu, X.-J.; Meng, J. Crystal structures and elastic properties of superhard IrN_2 and IrN_3 from first principles. *Phys. Rev. B* **2007**, *76*, 054115. [CrossRef]

44. Hill, R. The Elastic Behaviour of a Crystalline Aggregate. *Proc. Phys. Soc. A* **1952**, *65*, 349–354. [CrossRef]

45. Reuss, A. Berechnung der Fließgrenze von Mischkristallen auf Grund der Plastizitätsbedingung für Einkristalle. *Z. Angew. Math. Mech.* **1929**, *9*, 49–58. (In German) [CrossRef]

46. Hu, C.H.; Chen, D.M.; Wang, Y.M.; Yang, K. First-principles investigations of isotope effects in themodynamic properties of TiX_2 (X = H, D, and T) system. *J. Alloy. Comp.* **2008**, *450*, 369–374. [CrossRef]

47. Kelkar, T.; Kanhere, D.G.; Pal, S. First principles calculations of thermal equations of state and thermodynamical properties of MgH2 at finite temperatures. *Comput. Mater. Sci.* **2008**, *42*, 510–516. [CrossRef]

48. Fang, H.; Liu, B.; Liu, X.; Huang, S.; Ni, C.; Li, Z.; Wang, R. High-pressure lattice dynamic and thermodynamic properties of Ir by first-principles calculation. *Phys. B* **2010**, *405*, 732–737. [CrossRef]

49. Teter, D.M. Computational Alchemy: The Search for New Superhard Materials. *MRS Bull* **1998**, *23*, 22–27. [CrossRef]

50. Peng, F.; Chen, D.; Yang, X. First-principles calculations on elasticity of OsN_2 under pressure. *Solid State Commun.* **2009**, *149*, 2135–2138. [CrossRef]

51. Brazhkin, V.V.; Lyapin, A.G.; Popova, S.V.; Antonov, Y.V.; Kluev, Y.A.; Naletov, A.M. Mechanical Properties of the Superhard Polymeric and Disordered Phases Prepared From C_{60}, C_{70}, and C_{2N} under High Pressure. *Rev. High Pressure Sci. Technol.* **1998**, *7*, 989–991. [CrossRef]

52. Pugh, S.F. XCII. Relations between the elastic moduli and the plastic properties of polycrystalline pure metals. *Philos. Mag.* **1954**, *45*, 823–843. [CrossRef]

53. Morinaga, M.; Saito, J.; Yukawa, N.; Adachi, H. Electronic effect on the ductility of alloyed TiAl compound. *Acta Metall. Mater.* **1990**, *38*, 25–29. [CrossRef]

54. Song, Y.; Xu, D.S.; Yang, R.; Li, D.; Hu, Z.Q. Theoretical investigation of ductilizing effects of alloying elements on TiAl. *Intermetallics* **1998**, *6*, 157–165. [CrossRef]